Colloids and Surfaces B: Biointerfaces 103 (2013) 253–260

Contents lists available at SciVerse ScienceDirect

Colloids and Surfaces B: Biointerfaces

journal homepage: www.elsevier.com/locate/colsurfb

Model immunoassay on silicon surfaces: Vertical and lateral nanostructure vs. protein coverage

K. Awsiuk[a], A. Budkowski[a,*], P. Petrou[b], A. Bernasik[d], M.M. Marzec[d], S. Kakabakos[b], J. Rysz[a], I. Raptis[c]

[a] M. Smoluchowski Institute of Physics, Jagiellonian University, Reymonta 4, 30-059 Kraków, Poland
[b] Institute of Nuclear & Radiological Sciences & Technology, Energy & Safety, NCSR "Demokritos", End Patriarchou Gregoriou Str., 15310 Aghia Paraskevi, Greece
[c] Institute of Advanced Materials, Physicochemical Processes, Nanotechnology and Microsystems, NCSR "Demokritos", End Patriarchou Gregoriou Str., 15310 Aghia Paraskevi, Greece
[d] Faculty of Physics and Applied Computer Science, AGH-University of Science and Technology, Al. Mickiewicza 30, 30-059 Kraków, Poland

ARTICLE INFO

Article history:
Received 17 July 2012
Received in revised form 25 October 2012
Accepted 25 October 2012
Available online 3 November 2012

Keywords:
Immunoglobulins
Amino-organosilane films
Specific binding
Angle-resolved X-ray photoelectron spectroscopy
Atomic force microscopy
Time-of-flight secondary ion mass spectrometry

ABSTRACT

To provide complete characterization of immunoassay on silicon biosensor surfaces, atomic force microscopy, (angle-resolved) X-ray photoelectron spectroscopy and time-of-flight secondary ion mass spectrometry were applied to examine Si_3N_4 surfaces modified with (3-aminopropyl)triethoxysilane, coated with gamma globulins (IgG), blocked with bovine serum albumin and then reacted with anti-IgG antibody for two complementary pairs (rabbit and mouse IgG) at various concentrations (from 0.3 nM to 330 nM). Protein coverage, as reflected in (amine to total N1s) XPS signal ratio and determined from ARXPS, decreases slightly due to blocking and then increases monotonically for anti-IgG antibody concentrations higher than 1 nM. AFM images reveal hardly any change of lateral nanostructure due to blocking but response to antibody solutions, based on both the mean size (from autocorrelation) and dominant spacing (from Fourier analysis) of surface features, similar to that given by ARXPS. AFM height histograms provided information about the vertical nanostructure and the parameters of height distribution (average height, spread – roughness and skewness) were distinctly influenced by coating, blocking and immunoreaction. Average protein layer thickness values determined based on protein structure (molecular weight, dimensions) and surface coverage provided from ARXPS were in accord with average height of protein layer determined from AFM. TOF-SIMS analysis indicated that BSA blocks free surface sites and in addition replaces some already adsorbed IgGs.

1. Introduction

Due to the specificity and selectivity of recognition between antigen and antibody, immunoassays are exploited routinely in diagnostic laboratories. Recently, silicon-based micro- and nanofabrication technology has enabled construction of immunosensors, where the antigen–antibody binding takes place at the surface of silicon transducers [1–4]. To provide a suitable interface for the biomolecules, the silicon surface is frequently modified with amino-organosilanes [1,3]. After the immobilization of the specific recognition biomolecules, free surface sites are blocked, usually with non-functional proteins, to limit non-specific binding of targeted analytes [3,5–7].

Model antigen–antibody binding reactions between immobilized gamma globulins (IgG) and secondary anti-species specific antibody (anti-IgG) have been examined with atomic force microscopy [6,8–12]. Even a single specific recognition event has been discriminated from non-specific binding in situ by acquiring AFM images at the same spot before and after analyte injection [8]. In most of the AFM studies, however, the examined surfaces are covered with a large number of biomolecules, a situation more relevant to operative biosensors. Nevertheless, in all cases, the antigen–antibody complexes were characterized only *fragmentally* by the determined changes in either the average size [9,11] or the average height [6,10] of surface features manifested in AFM images (recorded in liquid [8,9] or air [6,10–12]).

In our previous work, in order to provide a more direct insight about biomolecular layers created onto biochips within multistep procedures, silicon surfaces have been examined with AFM in air after silanization, immobilization of IgG, blocking and specific binding reaction [6,11]. In addition, to allow for a more complete characterization, the local AFM analysis has been augmented with spectroscopic inspection [6,11,13]. For instance, lateral nanostructural features determined from AFM images (such as the mean size and dominant spacing of surface features) were supplemented with protein surface coverage, determined rigorously from analysis of the same surfaces with angle-resolved X-ray photoelectron spectroscopy (ARXPS) [11].

* Corresponding author. Tel.: +48 12 66 35 550; fax: +48 12 63 37 086.
E-mail address: ufbudkow@cyf-kr.edu.pl (A. Budkowski).

0927-7765/$ – see front matter © 2012 Elsevier B.V. All rights reserved.
http://dx.doi.org/10.1016/j.colsurfb.2012.10.047

In this work, we extend the above approach [11] to study two model *immunoassays*, based on recognition between anti-IgG antibody and the respective IgG, as a function of anti-IgG antibody concentration. In particular, rabbit or mouse IgGs have been immobilized onto aminosilane-modified silicon nitride surfaces and after blocking probed with the respective anti-species specific antibodies. AFM inspection revealed not only the lateral but also the *vertical* nanostructure of the biomolecule modified silicon surfaces. The AFM histograms of height distribution provided three measures of imaged surfaces, namely the distribution's mean value (average height), spread (roughness) and asymmetry (skewness). As it was expected, these measures were greatly influenced by the contributions of biomolecules attached to substrate after the successive immobilization, blocking and immunoreaction steps. Non-specific (e.g. blocking) and specific (effective immunoreaction) bindings were clearly distinguished. Together with the data about lateral nanostructure (from AFM) and protein surface density (from ARXPS), the experimental results provided a coherent picture of the biomolecules attachment and distribution onto silicon surfaces during the performance of immunoassays. In particular, it was found that the average thickness of organic overlayer predicted based on protein surface density calculated by analysis of ARXPS data correlates well with the average height of surface features determined by AFM, signifying the complementarily of these two methods for complex surfaces characterization. In addition, the data from time-of-flight secondary ion mass spectrometry (TOF-SIMS) revealed two separate processes taking place during the blocking step, i.e. BSA adsorption on the free surface sites complemented by desorption of IgG from the surface.

2. Materials and methods

2.1. Biosensor surface preparation for model immunoassay

The silicon substrates used are silicon wafers purchased from Montco Silicon Technologies, Inc. (Spring City, PA, USA). 3-Aminopropyl(triethoxysilane) (APTES), rabbit (rIgG; globulins Cohn Fraction I, II) and mouse (mIgG; globulins Cohn Fraction I, II) gamma-globulins, affinity purified polyclonal anti-rabbit IgG and anti-mouse IgG antibodies produced in goat against the whole molecule, and bovine serum albumin (BSA; Cohn Fraction V) were purchased from Sigma Chemical Co., St. Louis, MO, USA.

Silicon nitride (Si_3N_4) surfaces were obtained by deposition of a 1000-nm thick thermally grown silicon dioxide layer followed by deposition of a 150-nm thick silicon nitride layer. Cleaning and hydrophilization of the substrates were performed with oxygen plasma (using a reactive ion etcher) applied for 30 s under pressure of 10 mTorr and power of 400 W. The hydrophilized Si_3N_4 surfaces were then modified by immersion in 0.5% (v/v) aqueous APTES solution for 2 min, gentle washing with distilled water and curing for 20 min at 120 °C.

Model immunosensor surfaces were prepared in successive steps as follows: (a) coating with rabbit (rIgG) or mouse (mIgG) gamma-globulins through incubation with a 660 nM IgG solution (in addition, a 33 nM rIgG solution was used to complete the TOF-SIMS data) in 0.05 M phosphate buffer, pH 7.4, for 1 h at room temperature (RT), followed by washing with 0.05 M phosphate buffer, pH 7.4, and distilled water, and drying under nitrogen stream; (b) blocking of free-protein binding sites of the surface via immersion in a 10 mg/ml BSA solution in 0.05 M phosphate buffer, pH 7.4 (blocking solution), for 1 h at RT, followed by washing and drying as previously. The surfaces were then reacted with anti-IgG specific antibodies through incubation with anti-rabbit IgG or anti-mouse IgG antibody solutions (respectively for surfaces coated with rabbit or mouse IgG) in 0.05 M phosphate buffer, pH 7.4, containing 10 mg/ml BSA, for 1 h at RT. The surfaces were then washed with 0.05 M phosphate buffer, pH 7.4, containing 0.05% (v/v) Tween 20, and distilled water and dried under nitrogen stream.

The stability of gamma globulins adsorption onto APTES-modified silicon nitride surface, as well as the stability of immunocomplexes formed through reaction with antibodies against rabbit or mouse gamma globulins have been tested using fluorescently labeled reagents and submitting the surfaces to extensive washing and/or to chaotropic solutions. Our results indicate that both the immobilization of rabbit or mouse gamma globulins through adsorption and the subsequent coupling of species specific antibodies are extremely stable (data not shown).

2.2. AFM surface characterization and image analysis methods

The AFM imaging of silicon nitride surfaces corresponding to the different steps of model immunoassays has been performed in air using an Agilent 5500 microscope working in non-contact mode. AFM cantilevers (probe type PPP-FMR, Nanosensors) with force constant of 2 N/m, resonant frequency of 75 kHz, and AFM tips with standard beam shape and small radius (<7 nm) were used. The set point and gains were adjusted to obtain minimal noise and clear images of the analyzed surfaces. For each sample, topography and phase images were acquired simultaneously at several randomly chosen locations.

Surface vertical nanostructures were specified using the parameters of height distribution in a topographic AFM image, such as the average height, $\langle h \rangle$ (the distribution's mean), the root-mean square RMS roughness, R_q (the distribution's spread), and the skewness, R_{sk} (the distribution's asymmetry). In addition, lateral nanostructures were also described based on autocorrelation and Fourier analysis of topographic and phase images. The relevant parameters of surface features were provided by the doubled width-at-half-maximum, *2whm*, of radial averaged autocorrelation function (the feature's mean size) as well as the reciprocal of wave vector ($1/k$) at the maximum of radial averaged 2-dimensional fast Fourier transform (dominant spacing between the features). The vertical and lateral parameters were determined from AFM micrographs using the WSxM scanning probe microscopy software provided by Nanotec Electronica S.L. [14] (http://www.nanotec.es)

2.3. XPS and ARXPS surface characterization

X-ray photoelectron spectroscopy measurements were performed using a VSW Manchester spectrometer equipped with an Al Kα radiation source (1486.6 eV, 200 W). Angle-resolved XPS spectra were collected for three different values (0°, 60° and 70°) of photoelectron take-off angle Θ, which is defined as a angle between normal to the surface and the axis of the XPS analyzer lens. The operating pressure in the analytical chamber was less than 5×10^{-8} mbar. All XPS peaks were charge referenced to the neutral (C—C) carbon C 1s peak at 284.6 eV. Spectrum backgrounds were subtracted using the Shirley method. The aminosilane-organic bilayer model used to determine the thickness of APTES film and the amount (effective XPS thickness) of immobilized proteins has been described in details in our earlier publications [11,15].

2.4. TOF-SIMS surface characterization

To examine with TOF-SIMS the effect of blocking procedure as a function of initial surface coverage with rIgG, the samples were analyzed using the TOF.SIMS 5 (ION-TOF GmbH) instrument, equipped with a 30 keV bismuth liquid metal ion gun. Bi_3 clusters were used as the primary ions and the ion dose density was kept at levels lower than 10^{12} ion/cm^2 to ensure static mode conditions. High

mass resolution spectra were acquired from sample spots corresponding to areas of 100 μm × 100 μm. For all spectra the minimal mass resolution ($m/\Delta m$) at $C_4H_5^+$ ($m/z = 53$) peak was above 7400. Mass calibration was based on the H^+, H_2^+, CH^+, $C_2H_2^+$ and $C_4H_5^+$ peaks.

3. Results

All surfaces of Si_3N_4 substrate modified with (3-aminopropyl)triethoxysilane (APTES) were examined prior to and after each step of the model immunoassays involved in this study by AFM and ARXPS. The surfaces were coated with rabbit (or mouse) gamma-globulins (IgG), and non-specific binding was blocked with bovine serum albumin (BSA). Then the surfaces were exposed to solutions of anti-IgG antibody to allow for specific binding with the immobilized IgGs. In case of rabbit IgG/anti-rabbit IgG different concentrations of anti-IgG antibody ($0.3\ \text{nM} \le c \le 330\ \text{nM}$) have been used, whereas in case of mouse IgG/anti-mouse IgG a single antibody concentration ($c = 330\ \text{nM}$) was applied. If not otherwise stated, the results for the two complementary pairs are presented in the same plots as solid and open symbols for the rabbit and mouse the IgG, respectively.

3.1. Protein surface coverage reflected by XPS and determined from ARXPS

The multilayer structure silicon/APTES/protein of the silicon oxide and silicon nitride surfaces coated with IgG has been studied in our previous publication using XPS and ARXPS to examine the surfaces prior to and after both blocking with BSA and immunoreaction with anti-IgG antibody [11]. The mesoscopic uniformity of the protein overlayer has been also confirmed by near-field scanning optical microscopy [11]. Here, we apply photoelectron spectroscopy to evaluate, along with XPS, and determine in combination with ARXPS, surface coverage with protein of silicon nitride surfaces modified with an APTES film.

The XPS spectra of N1s core-level consist of both the signals characteristic for the Si_3N_4 substrate (binding energy of 397.5 eV) and for amine groups (NH_2, 399.8 eV, and protonated NH_3^+, 401.4 eV) present in the APTES/protein bilayer [11,15]. Therefore, the ratio of overlayer (NH_2 and NH_3^+) to total nitrogen concentration, N_{amine}/N, determined from XPS can be used as a measure of surface coverage by the bilayer. With the N_{amine}/N value for pure APTES film (6.8%) in mind, this ratio reflects also protein coverage. The N_{amine}/N ratio is plotted in Fig. 1a (left scale) as a function of secondary antibody concentration and compared with the situation prior to immunoreaction (labeled '+BSA' on the *x*-axis) and just after adsorption of gamma globulins (labeled 'IgG').

The ARXPS spectra depend on photoelectron take-of-angle Θ, that modifies sampling vertical depth, and on XPS thicknesses of APTES film (D) and protein layer (d), that justify the effective attenuation of photoelectrons (see the inset to Fig. 1b). The XPS thickness d, which is equivalent to a protein layer with uniformly distributed mass [11], is directly related (after being multiplied by protein density, 1.37 g/cm^3) with the density of proteins covering the surface.

The structural features of the APTES/protein bilayer are revealed by the ratio of intensities X_i of the photoelectrons characteristic for the aminosilane-organic bilayer (N1s from amine groups) and silicon substrate (Si 2p), that is plotted in a logarithmic form versus the take-off angle function $\sec\Theta$ (see Fig. 1b) [15]. The intensities X_i, calculated using tabulated sensitivity factors [16,17], are normalized with respect to molar fractions Z_i of the atoms emitting photoelectrons [11,15] (see the y-axis on Fig. 1b). The Z_i values for all used proteins (11%) have been determined in previous publications [11,15], while that for APTES and Si_3N_4 is obtained from the ARXPS data for the surface with no protein overlayer [11,15].

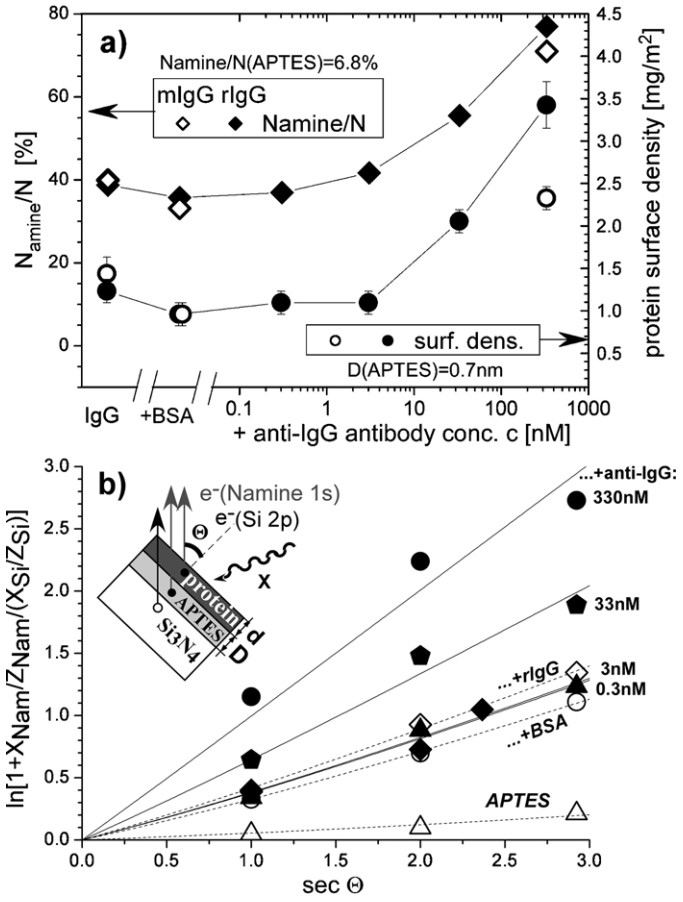

Fig. 1. (a) Protein coverage of silicon nitride surfaces expressed as the ratio of amine to total nitrogen concentration derived from the XPS N 1s spectrum (diamonds, left scale), and determined from ARXPS as protein surface density (circles, right scale) plotted against the anti-IgG antibody concentration c and compared with surfaces after IgG adsorption (labeled 'IgG') and blocking with BSA (zero antibody concentration). Solid and open symbols are for the series with rabbit and mouse IgG, respectively. (b) The ARXPS ratio of normalized intensities of photoelectrons characteristic for amino-organosilane/protein bilayer (N1s from NH_2 and NH_3^+) and Si_3N_4 (Si 2p) plotted versus the take-off angle function sec Θ. Lines mark results of linear regression analysis yielding XPS thickness of APTES and protein layer (D and d, respectively, marked in the inset). The latter, multiplied by protein density, yields protein surface density. The error bars for protein surface density (a) are given by the fitting procedure described in (b).

The data points, marked in Fig. 1b with different open and solid symbols, respectively, correspond to immunosensor-like surfaces after subsequent modification steps (silanization with APTES, immobilization of rabbit rIgG, blocking with BSA) as well as after exposure of those surfaces to solutions of different anti-rIgG concentrations (ranging from 0.3 nM to 330 nM). The slope of each individual data set, always starting at the origin of coordinate axes, depends on the total bilayer thickness (D with d). The thickness D of the APTES film, as determined in separate ARXPS measurements, is equal to 0.7 nm (in accord with previous results [11]). With the value of D known, the XPS thickness d of protein overlayer remains the only fitting parameter of the linear regression fitting equation [11,15]. The resulting values of protein coverage (surface density) are plotted in Fig. 1a (right scale) as a function of anti-IgG concentration and compared with the values after IgG adsorption (labeled 'IgG') and blocking with BSA (labeled '+BSA'), respectively.

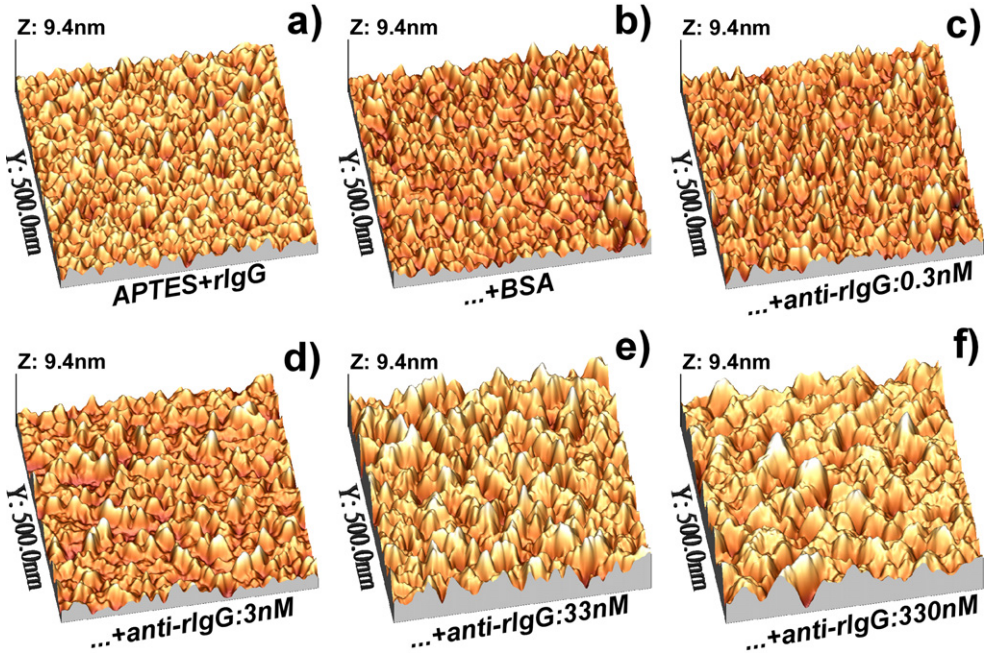

Fig. 2. Representative AFM topographic micrographs recorded for silanized Si_3N_4 after adsorption of rabbit IgG (a), blocking with BSA (b), and specific binding of anti-rabbit IgG antibody from solutions of different concentration *c* (c–f).

3.2. Immunosensor surfaces examined with AFM

The inner structure of the protein overlayers is revealed by topographic and phase AFM micrographs. Representative topography images recorded prior to and after the immunoreaction corresponding to the different concentrations of anti-rIgG antibody are shown in Fig. 2. The imaged protein overlayers can be described as random sets of surface features. Similar conclusions can be drawn for phase images (not presented).

3.2.1. Lateral nanostructure of protein overlayer

To examine quantitatively the lateral nanostructure of protein overlayer, autocorrelation and Fourier analysis was applied to the AFM micrographs, as suggested in our recent work [11]. The double of width at half-maximum, *2whm*, of radial averaged autocorrelation provides a measure of the mean size of topographic surface features. In addition, the reciprocal of wave vector at maximum, $(1/k)$, of radial averaged power spectrum provides a measure of the dominant spacing of the features observed in the topography and phase AFM images. The determined values of lateral measures of the inner structure of protein overlayer are presented in Fig. 3 (left scale for $(1/k)$, right scale for *2whm*) vs. the anti-IgG antibody concentration and in relation with the situations prior to immunoreaction (labeled '+BSA' on the *x*-axis) and just after adsorption of gamma globulins (labeled 'IgG').

3.2.2. Vertical nanostructure of protein overlayer

The vertical structure of surfaces examined with AFM is best described by the distribution of height in topographic images. Representative height histograms of AFM micrographs recorded prior to and after immunoreaction are shown (with their individual height scales) in Fig. 4a–c. The contributions from the molecules used for silanization and coating (IgG on APTES, Fig. 4a), blocking (BSA, Fig. 4b) and imunnoreaction (anti-IgG antibody, Fig. 4c) are illustrated schematically with separate Gaussian curves centered at different heights. These contributions change the overall height distribution in terms of its mean value, spread and asymmetry. Therefore, to characterize rigorously the vertical nanostructure of immunosensor-like surfaces, these three parameters are determined for each histogram: average height $\langle h \rangle$, standard deviation from $\langle h \rangle$ given by root mean square roughness R_q, and asymmetry specified by skewness R_{sk} (positive or negative for the longer histogram tail on its right or left side, respectively).

The mean values of these parameters as determined from the AFM height histograms are plotted in Fig. 5a and b against the anti-IgG antibody concentration and with respect to the situations prior to immunoreaction. In addition, the average height (left scale of Fig. 5a), RMS roughness (right scale of Fig. 5a) and skewness (Fig. 5b) can be also compared with the values corresponding to the silanized substrate with $\langle h \rangle = 0.83$ nm, $R_q = 0.22$ nm and zero R_{sk}, respectively.

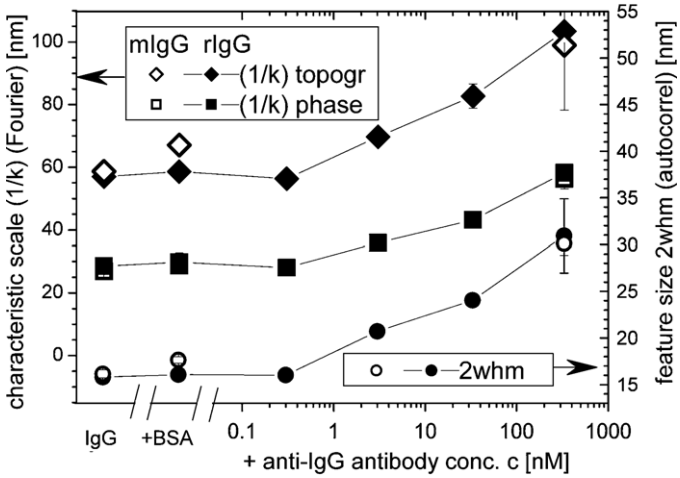

Fig. 3. Lateral nanostructure parameters of biomolecule modified Si_3N_4 surfaces. Characteristic spacing $(1/k)$ (left scale) and mean size of surface features *2whm* (right scale) determined from topography and phase contrast AFM images plotted as a function of antibody concentration *c* (solid and open symbols are for the series with rabbit and mouse IgG, respectively). The initial values correspond to IgG coated surface, while those at $x = 0$ to the blocked surface. Error bars are standard deviations, each determined from 5 images of the same surface.

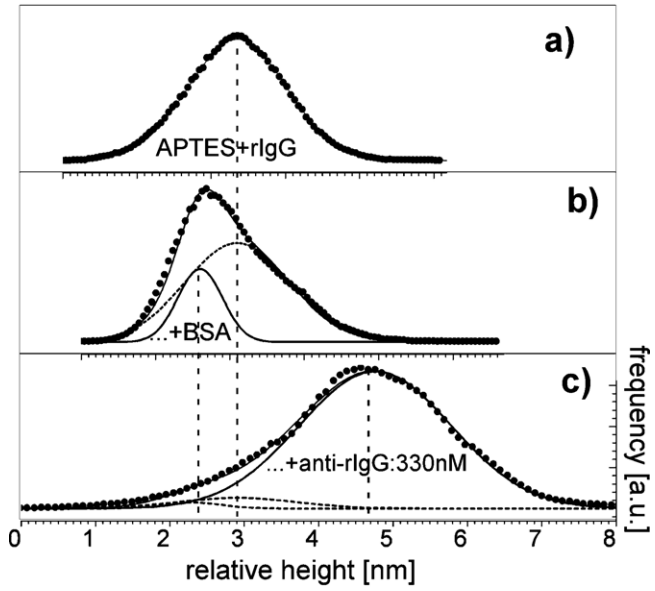

Fig. 4. Representative height histograms (with individual height scales) from AFM micrographs of Si_3N_4 substrates silanized with APTES after coating with rabbit IgG (a), blocking with BSA (b) and immunoreaction with anti-rabbit IgG antibody (330 nM) (c). Contributions due to rabbit IgG and APTES, BSA and anti-rabbit IgG antibody are illustrated schematically with separate Gaussian curves. Deviations from flat surfaces are characterized by average height $\langle h \rangle$, standard deviation from $\langle h \rangle$ (RMS roughness R_q), and asymmetry (skewness R_{sk}, positive or negative for longer right or left side tail of histogram, respectively).

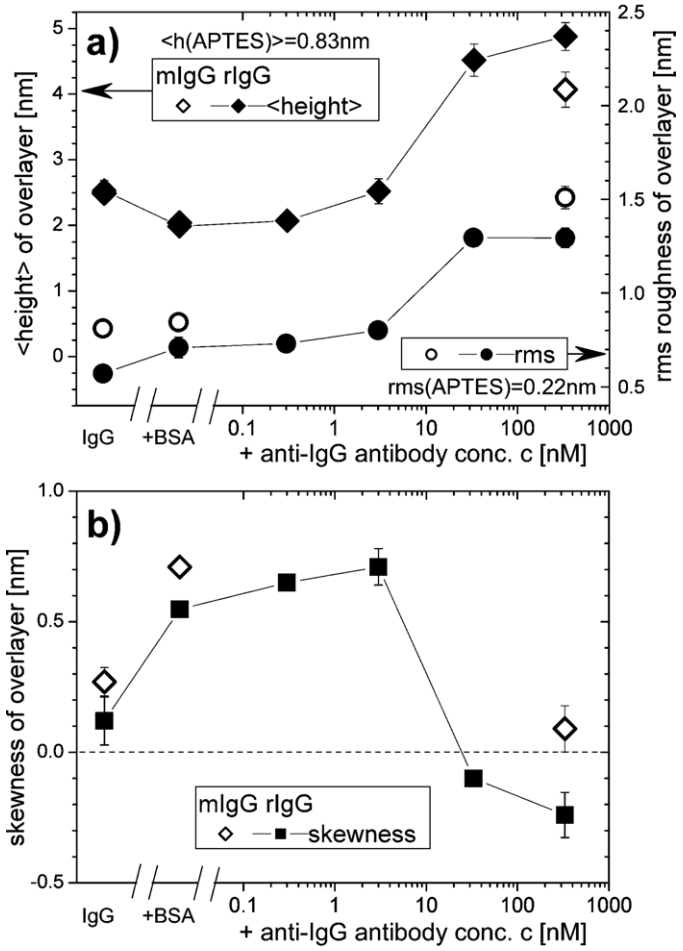

Fig. 5. Vertical nanostructure parameters of biomolecule modified Si_3N_4 surfaces as determined from AFM height histograms (see Fig. 4). Mean values of average height $\langle h \rangle$ (left scale in (a)), root mean square roughness R_q (right scale in (a)) and skewness R_{sk} (b) are plotted as a function of anti-IgG antibody concentration and compared with the initial value of IgG coated surface, and that corresponding to the blocked surface ($x = 0$). Error bars are standard deviations, each determined from 5 images.

4. Discussion

4.1. Biosensor surface prior to immunoassay

The surface modification with proteins through adsorption of gamma globulins to Si_3N_4 modified with APTES was quantified taking into account the substrate composition as specified by the molar fractions of silicon in the substrate, $Z_{Si} = 33.6 \pm 1.3\%$, and amine nitrogen in APTES film, $Z_{APTES} = 1.7 \pm 0.3\%$, determined by ARXPS. For the adsorbed rabbit and mouse IgG, the protein area density values determined by ARXPS were 1.25 ± 0.15 and 1.4 ± 0.2 mg/m^2, respectively (Fig. 1a). These values are comparable with the value of 1.1 ± 0.1 mg/m^2, determined in a previous publication [11] for rabbit IgG adsorbed to SiO_2 silanized with APTES, with $Z_{APTES} = 2.6 \pm 0.4\%$ and $Z_{Si} = 32.5 \pm 1.4\%$, respectively. This finding confirms earlier conclusions that the silicon substrate composition, either Si_3N_4 or SiO_2, has small impact on immunoglobulin adsorption [11]. The determined surface densities of adsorbed rabbit and mouse IgG (1.25–1.4 mg/m^2) are lower than the value expected for an area covered by singular immunoglobulin with side-on orientation (2.6 mg/m^2), while the other orientations (end-on, head-on) would result in even higher surface densities. This suggests partial but sizeable surface coverage with adsorbed IgGs with a side-on orientation that results in low surface coverage [18,19].

Adsorbed gamma globulins (rabbit or mouse IgG) form surface nanostructures (Fig. 2a), described as randomly distributed features corresponding to a topographic extent *2whm* of 16 nm (Fig. 3), comparable with the apparent IgG radii of 14 and 12 nm, respectively. These values are the adsorbed IgG radii predicted due to the broadening caused by the AFM tip (with 7 nm radius) for spherical [12] and half-spherical [9] molecular shapes (with 'real' radius of 7 nm [10]). For the Fc (or Fab) subunits of IgG ('real' radius of 4 nm [20]) the radii expected from both models are somewhat smaller (11 and 8 nm, respectively). On the other hand, the spacing ($1/k$) between the features (Fig. 3), obtained from topography (57–59 nm) is two times larger than that calculated from the phase images (27–29 nm). This suggests that topography AFM images show modulated height of immobilized IgG molecules, in accord with previous conclusions [11]. In addition, the spacing ($1/k$) determined by the phase images doubles the topographic size *2whm*. If the latter is related with the radius of IgG, then a picture of the surface with partial but sizeable coverage emerges in accord with the conclusion from surface coverage analysis.

The blocking procedure, which involves incubation of the surfaces coated with IgG with a high concentration BSA solution, reduces the surface coverage with proteins. This effect, visible already in the amine to total nitrogen concentration (Fig. 1a), is quantified based on ARXPS data (Fig. 1b) as a 33% and 22% reduction of the initial coverage of 1.4 mg/m^2 (mouse IgG) and 1.25 mg/m^2 (rabbit IgG), respectively. Taking into account previous results [11] that show hardly any change of total protein area density for surfaces with lower initial coverage (1.1 mg/m^2 of rabbit IgG), this finding suggests that the outcome of blocking with BSA depends on initial surface coverage with IgG. To further analyze this issue, we examined with TOF-SIMS surfaces modified with rabbit IgG through adsorption from solutions of two different concentrations (33 and 660 nM), both prior to and after blocking with BSA. The results are presented in Fig. 6 as uniform (after adsorption) and hatched (after blocking) columns, respectively, and correspond to the normalized intensities of specific secondary ions, characteristic

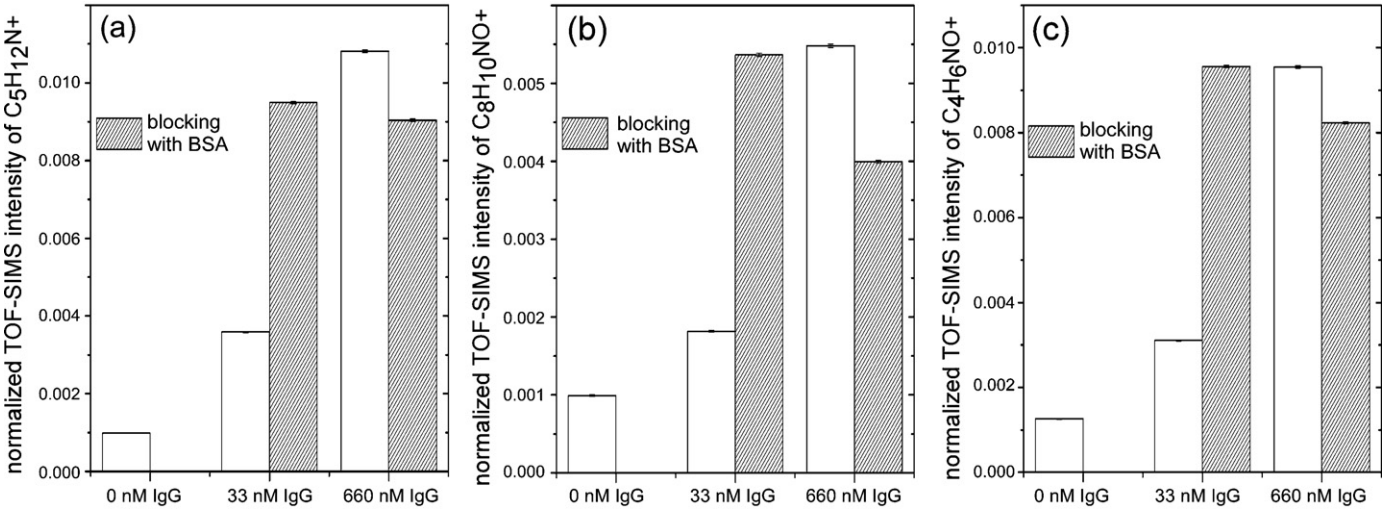

Fig. 6. TOF-SIMS intensities of secondary ions characteristic for proteins: (a) $C_5H_{12}N^+$ (from Ile and Leu [21,22]), (b) $C_8H_{10}NO^+$ (from Tyr [21,22]) and (c) $C_4H_6NO^+$ (from Glu and Gln [22]), normalized to the total ion intensity, as determined for Si_3N_4 surfaces silanized with APTES (reference values for 0 nM concentration) after rIgG adsorption from 33 nM and 600 nM solutions (uniform columns), respectively, and subsequent blocking with BSA (hatched columns). Error bars are standard deviations determined from the TOF-SIMS intensities.

for the amino acids [21,22] present both in IgG and BSA. While the surfaces with high rIgG coverage (obtained using a 660 nM solution for coating) show again blocking-induced reduction of total protein surface density, the surfaces with much lower initial coverage (obtained using a 33 nM rIgG solution for coating) manifest a huge increase of protein coverage upon exposure to BSA solution. This indicates two dominant processes taking place during blocking, BSA occupying mainly the free surface sites at surfaces with low coverage, and additionally replacing part of adsorbed IgG molecules at surfaces with higher protein density.

Recent experiments show that proteins can change their adsorption from irreversible to reversible, when a critical surface coverage is reached [23]. Similar behavior of IgG molecules in the presence of BSA solution is suggested for a critical coverage value of $\sim$1.1 mg/m^2. Above this value, the surface left by desorbed IgG molecules can be populated by BSA. IgG molecules (with nominal dimensions of 14.5 nm $\times$ 8.5 nm $\times$ 4 nm [10]) and BSA (with nominal dimensions of 14 nm $\times$ 4 nm $\times$ 4 nm [5]) can form monolayers of adsorbed molecules with side-on orientation and experimental thickness of 5 nm [5,19] and 4 nm [5], respectively. Since IgG and BSA are comparable in size except for one dimension, their partial exchange should lead to a visible reduction of total protein coverage accompanied by less distinct (vertical) change in surface nanostructure. In fact, hardly any effect on the three *lateral* structural scales is observed (see Fig. 3). Both the mean size *2whm* of topographic surface feature, and dominant spacing ($1/k$) of the features visible on topography and phase AFM images are not altered during blocking. However, the three parameters ($\langle h\rangle$, R_q, R_{sk}) of *vertical* nanostructure, determined from AFM histograms of height distribution (cf. Fig. 4a and b) are affected by blocking. In particular, the average height $\langle h\rangle$ is reduced (Fig. 5a, left scale), the distribution's spread (RMS roughness R_q) slightly increased (Fig. 5a, right scale), and the skewness R_{sk} increased from zero to positive values (Fig. 5b) – reflecting histograms with longer right-hand tails. The reason for all these changes in vertical nanostructure is the incorporation of smaller BSA molecules into IgG overlayer. The height distribution determined for immobilized BSA by surfaces coated directly with BSA is symmetric, with lower mean and spread values as compared to IgG. The schematic illustration of the BSA and IgG contributions in Fig. 4b explains their impact on height distribution after blocking. Intriguing relation between AFM height distribution, protein structure and surface coverage with proteins is discussed below in the Section 4.3.

4.2. Immunoassay on biosensor surface

Specific binding between immobilized IgG and anti-IgG antibody from solutions with increased concentration is manifested as a raise in protein coverage as it is presented in Fig. 1a with respect to the situation prior to immunoreaction (zero anti-IgG antibody concentration). Surface coverage with proteins, as detected by the changes in XPS (N 1s core level) signal ratio of N_{amine}/N, builds up with concentration c. These changes are visible for anti-rIgG concentrations equal to or higher than 3.3 nM. The ARXPS data, relying on angle-dependent ratio of XPS signals from different elements, seem less sensitive, since increase is observed for concentrations c equal to or higher than 33 nM. Nevertheless, the ARXPS data can provide the absolute values of protein area density which cannot be determined by XPS measurements [11,15]. For the rabbit IgG/anti-rabbit IgG antibody pair, the surface density of proteins increases from 1.1 ± 0.1 mg/m^2 to 3.4 ± 0.3 mg/m^2 as the antibody concentration increases from 0.3 nM to 330 nM. It should be noted that an area density of 2.4 mg/m^2 (reached at $c \sim 100$ nM) corresponds to a monolayer of densely packed (92% density) gamma globulin molecules with side-on orientation.

This monotonic increase of surface coverage with antibody concentrations equal to or higher than 3.3 nM (Fig. 1a) is accompanied by a similar increase of lateral nanostructure parameters (see Fig. 3). The mean size *2whm* of randomly distributed topographic features increases during immunoassay from 16.0 ± 0.2 nm to 30.9 ± 4.0 nm. In addition, the spacing ($1/k$) of the features, grows from 28.1 ± 0.7 nm to 58.3 ± 2.3 nm as determined by the phase AFM micrographs, and from 56.3 ± 1.5 nm to 103 ± 25 nm as determined by topography images. This approximately two-fold increase of the *2whm* value of surface features reflects a progressive formation of antigen–antibody complexes. Also, the characteristic scales ($1/k$) of both phase and topography images are roughly twice larger after immunoassay. Apparently, some of the imaged surface features must correspond to BSA or gamma globulins with orientations blocking or limiting the specific binding.

Immunoreaction of immobilized IgG with the anti-IgG antibody results also in drastic changes of vertical nanostructure. These changes are reflected in the parameters of the AFM height

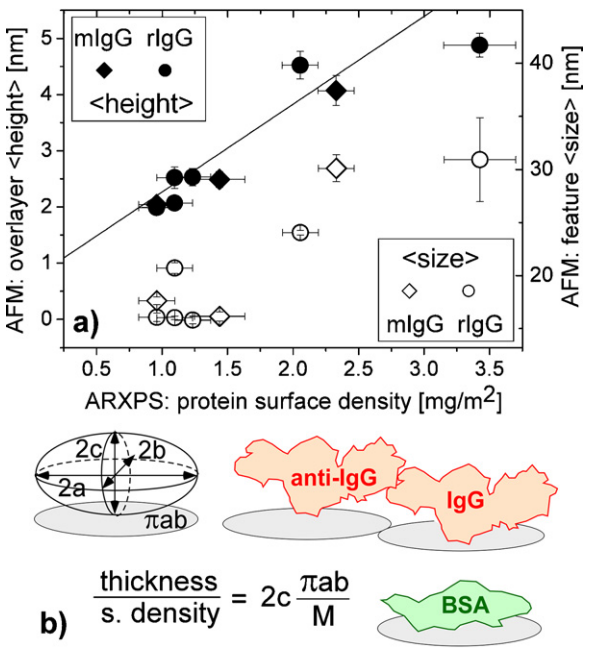

Fig. 7. (a) Vertical (average height ⟨*h*⟩, left scale) and lateral (mean feature size *2whm*, right scale) nanostructure parameters (from AFM) of Si_3N_4 surfaces coated with rabbit (circles) or mouse IgG (diamonds) plotted against protein surface density (from ARXPS). Solid line marks the average overlayer thickness expected from the model depicted in (b). Error bars are standard deviations, specified in Figs. 1 and 3.

histograms which are clearly modified after immunoreaction with antibody concentrations higher than 3.3 nM (Fig. 5). Such changes in the vertical structure are expected, since the antigen-binding sites of adsorbed gamma-globulins (with preferred side-on orientation) are located above the silanized silicon level (see sketch in Fig. 7b). In addition, the attached anti-IgG antibody molecules, in contrast to adsorbed immunoglobulins, are less prone to conformational modifications. There are two stages in the immunoassay-induced variation of vertical structure parameters (Fig. 5). First, the region of antibody concentration c up to 33 nM corresponds to a distinct increase in both the mean value (<*h*>) and spread (R_q) of height distribution accompanied by skewness R_{sk} reduced to zero. Second, for antibody concentrations equal to or higher than 33 nM a somewhat halted growth of both average height ⟨*h*⟩ and roughness R_q, and negative skewness are observed. The height histogram of AFM micrograph recorded for the rIgG modified surfaces after reaction with an anti-rIgG antibody solution of 330 nM is presented in Fig. 4c. We notice that the height distribution is dominated by the anti-IgG antibody contribution, with very small input from the adsorbed IgG and BSA (see outlined schematically Gaussian curves), resulting in longer left distribution's wing. This height histogram reveals also the critical point at which the AFM tip stops to penetrate the deeper regions of protein/APTES overlayer. This suggests complete formation of a continuous protein layer, expected from ARXPS to take place around $c \sim 100$ nM, when a side-on orientation of immobilized gamma-globulins is assumed.

4.3. Nanostructure vs. protein coverage

New insight into a model immunoassay on silicon nitride surfaces can be gained when the surface nanostructures, with their lateral and vertical parameters determined from AFM images and AFM height distributions, respectively, are analyzed as a function of surface coverage with proteins, evaluated by ARXPS. The results of such an analysis are presented in Fig. 7a for surfaces coated with rabbit (circles) or mouse IgG (diamonds). The plotted values of the mean size of surface features *2whm* (open symbols, right scale) show a monotonic albeit scattered relation with protein coverage, reflecting (except for two data points) progressive build up of antigen–antibody complexes. The high spread of values is mainly due to the two points with the lowest feature size, corresponding to adsorbed rabbit and mouse IgG, which upon blocking are shifted to the respective points with reduced abscissa (protein surface density) but almost the same ordinate (*2whm*).

More revealing is the relation between the average AFM height ⟨*h*⟩ and the surface coverage with proteins presented in Fig. 7a with solid symbols (left scale). The observed monotonic dependence can be correlated with the protein structure, i.e. the weight M of a single molecule and the dimensions $2a \times 2b \times 2c$ of ellipsoid describing the immobilized molecules shape. The ratio of globular thickness to molecular surface density is expressed as $2c\,(\pi ab/M)$ (see Fig. 7b). Please note that this formula is independent of immobilized protein orientations, as all ellipsoid dimensions are in its numerator. In addition, the ratio of thickness to area weight density calculated for immunoglobulin (IgG and anti-IgG, with 150 kDa molecular weigh), 1.69 nm m^2/mg, is almost the same as that of BSA (with 66.4 kDa molecular weigh), 1.73 nm m^2/mg. Therefore, practically one value characterizes all types of biomolecules present at the silicon surface. This ratio multiplied by the surface density corresponding to the area covered with a single protein (with given orientation) would provide the relevant globular thickness. In addition, this ratio multiplied by the actual surface coverage with proteins yields the average thickness of the protein layer. The predicted values, after the addition of the APTES film thickness (known from ARXPS) are presented as a solid line in Fig. 7a. This line matches quite well with the average AFM height ⟨*h*⟩ data (solid symbols), except for the last point which corresponds to anti-rIgG antibody concentrations higher than 100 nM, where AFM tips stops to penetrate the continuous protein/APTES overlayer.

5. Conclusions

To conclude, combined local microscopic (AFM) and global spectroscopic (XPS, ARXPS) analysis of biosensor-like surfaces (silicon modified with amino-organosilane APTES) has been extended to all the steps of an *immunoassay*, using antibody concentrations extending over four orders of magnitude ($0.3\ \text{nM} \le c \le 330\ \text{nM}$, for two complementary IgG/anti-IgG antibody pairs).

AFM detection of specific binding at biosensor-like surfaces with large number of biomolecules can be quantified by autocorrelation and Fourier analysis of AFM topography and phase images in terms of lateral nanostructure parameters. Following this approach, the formation of antigen–antibody complexes is detected for antibody concentrations equal to or higher than 3.3 nM. Similar sensitivity was demonstrated by XPS. ARXPS seems less sensitive (signals statistically different from zero antibody concentration are obtained for concentrations $c > 33$ nM) but on the other hand it can provide information about absolute surface coverage (area density) with proteins that the other two methods cannot.

In addition, the AFM height distribution parameters (mean – average height ⟨*h*⟩, spread – roughness R_q and asymmetry – skewness R_{sk}) provide complete, often neglected, information on *vertical* nanostructure that enables additional analysis of the biosensor-like surfaces prior to and after immunoreaction. These parameters resolve non-specific binding, due to blocking with BSA, from specific binding due to antigen–antibody interactions for concentrations higher than 1 nM.

Synergic examination of nanostructure and protein coverage, especially the relation of average AFM height vs. the protein surface

density, enables surface analysis involving protein dimensions but also weight of a single molecule. The average protein layer thickness determined taking into account both the protein structure and surface coverage is in accordance with average AFM height.

Spectroscopic examination (TOF-SIMS) of biosensor-like surfaces prior to immunoassay indicates that BSA not only blocks free surface sites but in addition replaces some adsorbed IgGs especially at the surfaces with high protein coverage.

Acknowledgments

This work was supported by the EU funded project "PYTHIA" (FP7-ICT2-224030), equipment purchased thanks to the financial support of the European Regional Development Fund (POIG.02.01.00-12-023/08).

References

[1] Y. Cui, Q. Wei, H. Park, C.M. Lieber, Science 293 (2001) 1289.
[2] R. Raiteri, M. Grattarola, H.-J. Butt, P. Skládal, Sens. Actuators B 79 (2001) 115.
[3] Q. Meskini, A. Abdelghani, A. Tlili, R. Mgaieth, N. Jaffrezic-Renault, C. Martelet, Talanta 71 (2007) 1430.
[4] E.F. Schipper, A.M. Brugman, C. Dominguez, L.M. Lechuga, R.P.H. Kooyman, J. Greve, Sens. Actuators B 40 (1997) 147.
[5] Y.L. Jeyachandran, J.A. Mielczarski, E. Mielczarski, B. Rai, J. Colloid Interface Sci. 341 (2010) 136.
[6] M. Kitsara, P. Petrou, D. Kontziampasis, K. Misiakos, E. Makarona, I. Raptis, K. Beltsios, Microelectron. Eng. 87 (2010) 802.
[7] J.S. Yuk, M. Trnavsky, C. McDonagh, D. MacCraith, Biosens. Bioelectron. 25 (2010) 1344.
[8] L. Li, S. Chen, S. Oh, S. Jiang, Anal. Chem. 74 (2002) 6017.
[9] Z.J. Lv, J.H. Wang, G.P. Chen, L.H. Deng, Int. J. Biol. Macromol. 47 (2010) 661.
[10] K.-B. Lee, S.-J. Park, C.A. Mirkin, J.C. Smith, M. Mrksich, Science 295 (2002) 1702.
[11] K. Awsiuk, A. Bernasik, M. Kitsara, A. Budkowski, P. Petrou, S. Kakabakos, S. Prauzner-Bechcicki, J. Rysz, I. Raptis, Colloids Surf. B 90 (2012) 159.
[12] O. Ouerghi, A. Touhami, A. Othmane, H. Ben Ouada, C. Martelet, C. Fretigny, N. Jaffrezic-Renault, Biomol. Eng. 19 (2002) 183.
[13] Y.M. Bae, B.-K. Oh, W. Lee, W.H. Lee, J.-W. Choi, Biosens. Bioelectron. 21 (2005) 103.
[14] I. Horcas, R. Fernandez, J.M. Gomez-Rodriguez, J. Colchero, J. Gomez-Herrero, A.M. Baro, Rev. Sci. Instrum. 78 (2007) 013705.
[15] K. Awsiuk, A. Bernasik, M. Kitsara, A. Budkowski, J. Rysz, J. Haberko, P. Petrou, K. Beltsios, J. Raczkowska, Colloids Surf. B 80 (2010) 63.
[16] J.H. Scofield, J. Electron. Spectrosc. 8 (1976) 129.
[17] D. Briggs, Surface Analysis of Polymers by XPS and Static SIMS, Cambridge Univ. Press, Cambridge, 1998.
[18] H. Urano, S. Fukuzaki, J. Biosci. Bioeng. 90 (2000) 105.
[19] A. Tronin, T. Dubrovsky, C. Nicolini, Langmuir 11 (1995) 385.
[20] J. Buijs, J.W. Lichtenberg, W. Norde, J. Lyklema, Colloids Surf. B 5 (1995) 11.
[21] M. Dubey, K. Emoto, H. Takahashi, D.G. Castner, D.W. Grainger, Adv. Funct. Mater. 19 (2009) 3046.
[22] H. Wang, D.G. Castner, B.D. Ratner, S. Jiang, Langmuir 20 (2004) 1877.
[23] M. Rabe, D. Verdes, M. Rankl, G.R.J. Artus, S. Seeger, ChemPhysChem 8 (2007) 862.